Journal of Innovative Applied Mathematics and Computational Sciences

J. Innov. Appl. Math. Comput. Sci. **5**(1) (2025), 31–52. DOI: 10.58205/jiamcs.v5i1.1928

http://jiamcs.centre-univ-mila.dz/

Stability and sensitivity analysis of an infectious respiratory disease with vaccination and use of face masks

Henry Milimo Wanjala ✉[1], Mark O. Okongo [1] and Jimrise O. Ochwach [2]

[1]Department of Physical Sciences, Chuka University, Nairobi - Meru Higway, Chuka, 60400, kenya
[2]Department of Computing & Information Technology, Mama Mama Ngina University College, off Mutomo - thangari road, 01030, Kenya

Received April 14, 2025, Accepted June 13, 2025, Published July 6, 2025

Abstract. Mathematical modeling serves as a vital tool in public health, enabling policymakers to synthesize evidence, forecast disease trends, and assess intervention strategies. This study investigated the combined effects of face masks, quarantine, social distancing, and vaccination in controlling infectious respiratory diseases. The reproduction number was derived using the next-generation matrix (NGM). Local stability analysis utilized the Gershgorin Circle Theorem, while global stability was analyzed through the Quadratic Lyapunov Theorem. Sensitivity analysis was conducted using the normalized forward sensitivity index, and numerical simulations were performed with Python libraries such as *scipy*, *numpy*, and *matplotlib.pyplot*. Bifurcation analysis was carried out using the Center Manifold Theorem. The findings revealed that while these measures effectively reduced infection spread, they were insufficient to completely eliminate disease transmission. This study underscores the importance of implementing multiple strategies concurrently to effectively control the transmission of infectious diseases and guide public health interventions.

Keywords: Disease Modelling, Face-Masks, Vaccination, Stability Analysis, Bifurcation Analysis, Sensitivity Analysis.

2020 Mathematics Subject Classification: 34D20, 37G15, 34C60, 92B05, 92D30. MSC2020

1 Introduction

Mathematical modelling has proven to be a valuable tool for policymakers, helping them synthesize evidence, forecast outcomes, plan interventions, and evaluate decisions. According to [15], these models are essential for proactively preventing, predicting, and mitigating disease transmission. As [23] highlights, the primary goals in controlling respiratory infectious

✉Corresponding author. Email: milhenry61@gmail.com

ISSN (electronic): 2773-4196

diseases are to reduce infection rates and manage the strain on healthcare systems and personnel. Researchers have proposed various mathematical models to analyze the dynamics of infectious respiratory diseases, aiding in predicting outbreaks and exploring control strategies. A key aspect of these models is the reproduction number, which helps to understand the nonlinear dynamics of disease transmission.

One effective way to control outbreaks is by developing and distributing vaccines on a large scale. Vaccination can provide temporary or even lifelong immunity, preventing susceptible individuals from becoming infected [19]. A study by [5] developed a model to examine the risk of infection spread, the peak prevalence, and the timing of the peak. Their findings suggested that COVID-19 cannot be entirely eradicated through vaccination alone. Instead, vaccination may lead to a milder but prolonged epidemic unless additional non-pharmaceutical interventions (NPIs) are implemented. Similarly, [21] proposed a SEIHR model with and without impulsive vaccination strategies, demonstrating that impulsive vaccination could significantly accelerate disease containment. The study by [2] also found that vaccination could prevent outbreaks when the reproduction number is reduced to less than one.

In addition to vaccination, non-pharmaceutical interventions (NPIs) are essential in curbing the transmission of respiratory infections. These include measures such as quarantine, isolation, and use of face masks. NPIs are community-level actions designed to slow infection spread during epidemics [11]. For example, [3] developed a mathematical model that highlighted the critical role of quarantine. Their study concluded that detecting and isolating infected individuals early is crucial for controlling COVID-19 spread. The study by [14] showed that combining vaccination with quarantine significantly reduced infections, while the absence of these measures led to a rapid increase in cases.

Face masks are another key tool in preventing respiratory infections. There are three main types: respirators, used primarily in healthcare settings; surgical masks, employed in both medical and community contexts; and cloth masks, commonly used in communities [17]. Authors in [24] found that the effectiveness of face masks depends on their efficiency and consistent, proper use both of which are crucial and interdependent factors. Despite their importance, public resistance to wearing masks remains a challenge. However, masks are particularly effective in limiting the spread of infection from asymptomatic individuals or those not yet diagnosed [16]. Notably, populations in Asian countries, with prior experience in handling coronavirus epidemics, exhibit less resistance to mask usage [8].

While these studies provide valuable insights into individual interventions, few models simultaneously account for the combined effects of vaccination, face-mask usage, and quarantine in a unified framework. This forms the main motivation for this study. In real-world settings, such interventions are often implemented together, and their joint effect on disease transmission and control is not always linear or additive. Understanding the synergy between these control strategies is crucial for designing effective public health policies, particularly in resource-limited settings where optimizing intervention combinations is essential.

The novelty of this study lies in developing a deterministic compartmental model that simultaneously incorporates vaccination, face-mask use, and quarantine, followed by rigorous stability and sensitivity analysis. While previous studies have investigated these interventions separately or in pairs, our model integrates them into a comprehensive framework. Additionally, we conduct both local and global stability analyses of the disease-free equilibrium and perform a sensitivity analysis to determine the most influential parameters affecting the reproduction number.

Our methodological approach differs from other modelling studies in that we utilize both

analytical and numerical tools, including the next-generation matrix method for calculating the basic reproduction number and sensitivity analysis using normalized forward sensitivity indices. This combination allows us to not only assess the stability of the disease-free equilibrium but also identify key levers for effective intervention strategies.

Nonetheless, this study has certain limitations. The model assumes homogeneous mixing of the population and does not account for age structure, spatial heterogeneity, or stochastic effects. Furthermore, the efficacy of interventions like vaccination and mask usage is assumed constant over time, which may not hold true in real-world scenarios where compliance and immunity can wane.

In summary, this study aims to evaluate the effectiveness of face masks, quarantine, and vaccination as strategies for preventing and reducing the transmission of infectious respiratory diseases. By providing a unified model and analyzing its stability and sensitivity characteristics, we offer important insights into how combined interventions can be optimized for better disease control.

2 Model formulation and development

The total human population at a given time t, denoted by $N(t)$, is compartmentalised into eight mutually exclusive sub-populations: susceptible ($S(t)$), vaccinated ($V(t)$), exposed ($E(t)$), quarantined ($Q(t)$), asymptomatic but infectious ($A(t)$), symptomatic but infectious ($I(t)$), isolated ($J(t)$) through hospitalisation or specialised care, and recovered ($R(t)$).

The total human population is therefore given by:

$$N(t) = S(t) + V(t) + E(t) + Q(t) + A(t) + I(t) + J(t) + R(t). \tag{2.1}$$

The mathematical model governing the transmission dynamics of the infectious disease is described by the following system of deterministic non-linear differential equations:

$$\begin{aligned}
\frac{dS}{dt} &= \Lambda + (1-d)zQ + \delta R - (\alpha + \lambda + \mu)S, \\
\frac{dV}{dt} &= \alpha S - (\mu + (1-\theta)\lambda)V, \\
\frac{dE}{dt} &= \lambda S + (1-\theta)\lambda V - (\mu + g + c)E, \\
\frac{dQ}{dt} &= cE - (\mu + z)Q, \\
\frac{dA}{dt} &= fgE - (\mu + r_1)A, \\
\frac{dI}{dt} &= (1-f)gE - (\mu + r_2 + \eta)I, \\
\frac{dJ}{dt} &= \eta I + dzQ - (\mu + r_3)J, \\
\frac{dR}{dt} &= r_1 A + r_2 I + r_3 J - (\mu + \delta)R.
\end{aligned} \tag{2.2}$$

The force of infection, λ, is given by:

$$\lambda = \beta(1 - \epsilon_m c_m)(1 - S)(A + \epsilon_1 I + \epsilon_2 J)/N. \tag{2.3}$$

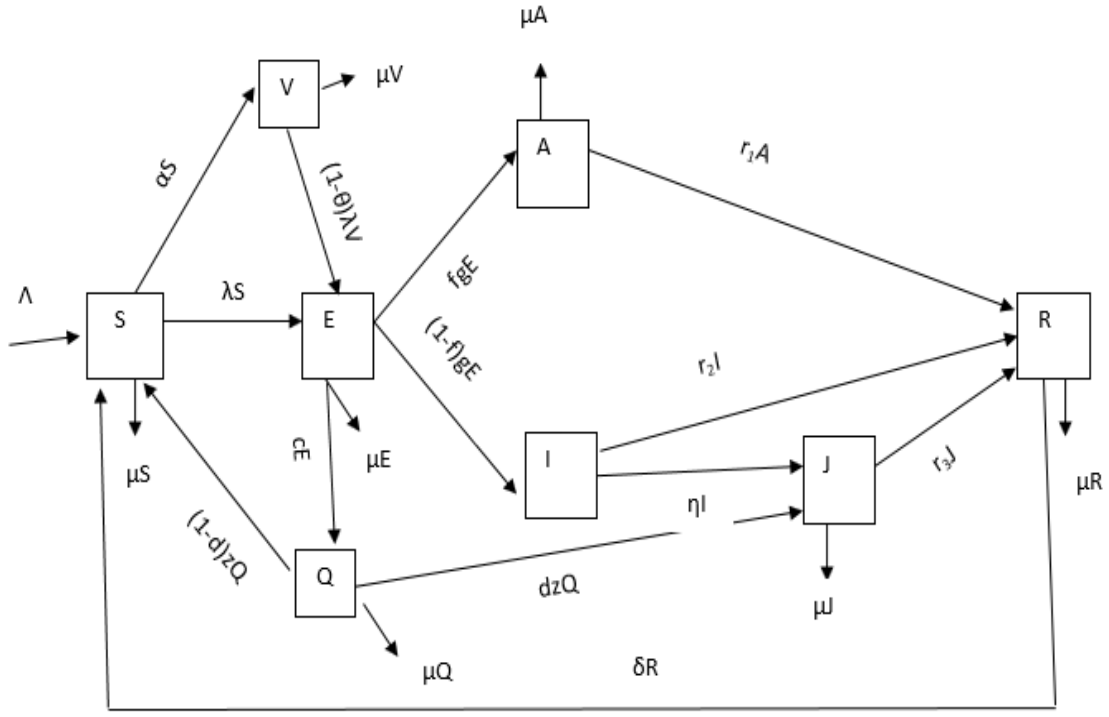

Figure 2.1: Model flow chart.

The model flow chart is shown in Figure 2.1.

The susceptible population grows at a rate Λ solely through births. A portion of the susceptible population is vaccinated at a rate α as part of a vaccination drive. However, the vaccine does not provide complete immunity; its efficacy, denoted by θ, ranges from $0 \leq \theta \leq 1$, where $\theta = 0$ implies no protection and $\theta = 1$ implies full protection against the virus. Susceptible individuals become infected at a rate determined by the force of infection, λ.

Through contact tracing, exposed individuals are quarantined at a rate c. After a quarantine period of z, a fraction d of those who are positive are isolated, while the remainder, who test negative, return to the susceptible class. Following a latency period of g, a fraction f of the exposed population becomes asymptomatic, while the rest exhibit symptoms.

Asymptomatic individuals recover at a rate r_1, whereas symptomatic individuals recover at a rate r_2. A subset of symptomatic individuals require specialised care in hospitals at a rate η, and these hospitalised individuals subsequently recover at a rate r_3. Recovered individuals gradually lose immunity at a natural rate δ. Additionally, there is a natural mortality rate μ across all compartments.

The model parameters and their values are presented in Table 2.1.

Symbol	Parameter	Value	Source
Λ	Recruitment rate by birth	0.46436 day^{-1}	[24]
μ	Natural death rate	4.563×10^{-5} day^{-1}	[23]
α	Vaccination rate	8.157×10^{-7} day^{-1}	[18]
d	Fraction of those isolated after quarantine	0.05	[16]
z	Quarantine period	0.0714 day	[23]
c	Quarantine rate	0.07 day^{-1}	[1]
f	Fraction of asymptomatic individuals	0.7	[23]
r_1	Recovery rate of asymptomatic individuals	0.0714 day^{-1}	Assumed
r_2	Recovery rate of symptomatic individuals	$\frac{1}{21}$ day^{-1}	Assumed
r_3	Recovery rate of hospitalised individuals	0.02 day^{-1}	Assumed
η	Rate of symptomatic individuals being hospitalised	0.94 day^{-1}	[20]
δ	Rate of loss of immunity	0.0033 day^{-1}	[12]
β	Effective contact rate	0.512 day^{-1}	[13]
$\epsilon_{1,2}$	Relative infectiousness of symptomatic/hospitalised individuals	0.48	[23]
ϵ_m	Efficacy of face masks	0.5	[24]
c_m	Consistency in using face masks	0.1	[24]
θ	Vaccine efficacy	0.8	Assumed
η_a	Fraction of asymptomatic but infectious individuals	0.7	[23]
s	Social distancing effectiveness	$0 \leq s \leq 1$	-

Table 2.1: Model parameters and their values.

3 Model analysis

3.1 Positivity of the solution

The model system (2.2) represents living organisms; hence, the corresponding state variables remain non-negative for all $t > 0$. Therefore, the solutions to model (2.2) with positive initial conditions remain positive for all $t > 0$.

Theorem 3.1. *The region* $\mathcal{D} = \{(S(t), V(t), E(t), Q(t), A(t), I(t), J(t), R(t)) \in \mathbb{R}^8_+ : N(t) \leq \frac{\Lambda}{\mu}\}$ *is positively invariant and attracting with respect to model (2.2).*

Proof. Solving the first equation of (2.2) for $S(t)$ at time $t > 0$, we obtain:

$$\begin{aligned}
\frac{dS}{dt} &= \Lambda + (1-d)zQ + \delta R - (\lambda + \mu + \alpha)S \\
\frac{dS}{dt} &\geq -(\lambda + \mu + \alpha)S \\
\int \frac{dS}{S} &\geq -\int (\lambda + \mu + \alpha)\, dt \\
\ln S - \ln S(0) &\geq -\int (\lambda + \mu + \alpha)\, dt \\
\ln \frac{S}{S(0)} &\geq -\int (\lambda + \mu + \alpha)\, dt \\
\frac{S}{S(0)} &\geq e^{-\int (\lambda+\mu+\alpha)\, dt} \\
S &\geq S(0)e^{-\int (\lambda+\mu+\alpha)\, dt}.
\end{aligned}$$

Clearly, $S(0)e^{-\int (\lambda+\mu+\alpha)\, dt}$ is a non-negative function of t, thus $S(t)$ remains positive. Equivalent arguments can be made to confirm the positivity of the other variables by utilising their corresponding equations. This indicates that the solutions to System (2.2), starting with non-negative initial conditions such that $V(t) > 0$, $E(t) > 0$, $Q(t) > 0$, $A(t) > 0$, $I(t) > 0$, $J(t) > 0$, and $R(t) > 0$, will remain non-negative for all $t \geq 0$. □

3.2 Invariant region

Theorem 3.2. *For the initial conditions* $S(0) = S_0 > 0$, $V(0) = V_0 > 0$, $E(0) = E_0 > 0$, $Q(0) = Q_0 > 0$, $A(0) = A_0 > 0$, $I(0) = I_0 > 0$, $J(0) = J_0 > 0$, *and* $R(0) = R_0 > 0$, *the solution of system (2.2) is contained in the region* $\mathcal{H} \subset \mathbb{R}^8_+$, *defined by*

$$\mathcal{H} = \left\{ [S(t), V(t), E(t), Q(t), A(t), I(t), J(t), R(t)] \in \mathbb{R}^8_+ : N(t) \leq \frac{\Lambda}{\mu} \right\}. \tag{3.1}$$

Proof. Summing all the equations of the model system (2.1) gives:

$$\frac{dN(t)}{dt} = \frac{dS(t)}{dt} + \frac{dV(t)}{dt} + \frac{dE(t)}{dt} + \frac{dQ(t)}{dt} + \frac{dA(t)}{dt} + \frac{dI(t)}{dt} + \frac{dJ(t)}{dt} + \frac{dR(t)}{dt}. \tag{3.2}$$

The change in the total population is defined by

$$\frac{dN}{dt} = \Lambda - \mu N, \tag{3.3}$$

which implies

$$\frac{dN}{dt} \leq \Lambda - \mu N. \tag{3.4}$$

Integrating equation (3.4) using the method of separation of variables and taking $N(0) = N_0$, the solution is given by

$$N(t) \leq \frac{\Lambda}{\mu} - \left(\frac{\Lambda}{\mu} - N_0\right) e^{-\mu t}, \quad \text{where } N_0 = N(0). \tag{3.5}$$

The work of [4] established the Birkhoff-Rota theorem, which states that if $N_0 < \frac{\Lambda}{\mu}$, then $N(t) \to \frac{\Lambda}{\mu}$ asymptotically as $t \to \infty$ in equation (3.1). Furthermore, the total population size satisfies $0 \leq N(t) \leq \frac{\Lambda}{\mu}$ for all $t \geq 0$. Consequently, all feasible solutions of the model remain within the region $\mathcal{H}$. □

3.3 Basic reproduction number

The basic reproduction number ($\mathcal{R}_0$) serves as a measure of the average number of secondary infections caused by a single infectious individual in a completely susceptible population.

The reproduction number $\mathcal{R}_0$ is determined using the Next Generation Matrix (NGM) method. This involves the Jacobian matrix, derived from the model's equations, which plays a key role in the computation of $\mathcal{R}_0$.

Theorem 3.3. *The basic reproduction number ($\mathcal{R}_0$) for the epidemiological model (2.2) is given by equation (3.6):*

$$\mathcal{R}_0 = \frac{m\beta_0(cdz\epsilon_2 k_3 k_4 - k_2(fgk_4k_5 - (1-f)gk_3(k_5\epsilon_1 - \eta\epsilon_2)))}{k_1k_2k_3k_4k_5}, \tag{3.6}$$

where

$$\begin{aligned} &m = \frac{\Lambda}{\mu}, \quad \beta_0 = \beta(1-\epsilon_m c_m)(1-s), \\ &k_1 = -(\mu + g + c), \quad k_2 = -(\mu + (1-d)z), \quad k_3 = -(\mu + r_1), \\ &k_4 = \mu + r_2 + \eta, \quad k_5 = \mu + r_3. \end{aligned}$$

Proof. The basic reproduction number is defined as the spectral radius of the matrix product FV^{-1}. To compute this, we isolate the infectious subsystem from model system (2.2) and derive the transmission matrix F and the transition matrix V, as given in equations (3.7) and (3.8):

$$F = \begin{pmatrix} 0 & 0 & m\beta_0 & m\beta_0\epsilon_1 & m\beta_0\epsilon_1 \\ 0 & 0 & 0 & 0 & 0 \\ 0 & 0 & 0 & 0 & 0 \\ 0 & 0 & 0 & 0 & 0 \\ 0 & 0 & 0 & 0 & 0 \end{pmatrix} \tag{3.7}$$

and

$$\mathcal{V} = \begin{pmatrix} k_1 & 0 & 0 & 0 & 0 \\ c & k_2 & 0 & 0 & 0 \\ fg & 0 & k_3 & 0 & 0 \\ (1-f)g & 0 & 0 & k_4 & 0 \\ 0 & dz & 0 & \eta & k_5 \end{pmatrix} \tag{3.8}$$

Then, the matrix product FV^{-1} is given by:

$$FV^{-1} = \begin{pmatrix} \mathcal{R}_0 & \frac{m\beta_0\epsilon_2 dz}{k_2k_5} & \frac{m\beta_0}{k_3} & -\frac{m\beta_0(\epsilon_1k_5-\eta\epsilon_2)}{k_4k_5} & -\frac{m\beta_0\epsilon_2}{k_5} \\ 0 & 0 & 0 & 0 & 0 \\ 0 & 0 & 0 & 0 & 0 \\ 0 & 0 & 0 & 0 & 0 \\ 0 & 0 & 0 & 0 & 0 \end{pmatrix} \tag{3.9}$$

Thus, the basic reproduction number is as given in equation (3.10):

$$\mathcal{R}_0 = \frac{m\beta_0(cdz\epsilon_2k_3k_4 - k_2(fgk_4k_5 - (1-f)gk_3(k_5\epsilon_1 - \eta\epsilon_2)))}{k_1k_2k_3k_4k_5}. \tag{3.10}$$

□

3.4 Equilibrium analysis

3.4.1 Disease-free equilibrium point

The Disease-Free Equilibrium (DFE) for system (2.2) is attained when all infection-related compartments are set to zero. This leads to the DFE given in equation (3.11):

$$\begin{aligned} \mathcal{E}_0 &= (S^0, V^0, E^0, Q^0, A^0, I^0, J^0, R^0) \\ &= \left(\frac{\Lambda}{\mu}, \frac{\alpha\Lambda}{\mu^2}, 0, 0, 0, 0, 0, 0\right). \end{aligned} \tag{3.11}$$

3.4.2 Stability analysis of the disease-free equilibrium point

Theorem 3.4. ***(Gershgorin Circle Theorem)*** *Let A be an $n \times n$ matrix with real entries. If the diagonal elements a_{ii} of A satisfy*

$$a_{ii} < r_i,$$

where

$$r_i = \sum_{\substack{j=1 \\ j\neq i}}^{n} |a_{ij}|,$$

for $i = 1, \ldots, n$, then all the eigenvalues of A are negative or have negative real parts.

The following corollaries will be used in the analysis of the equilibrium points of the proposed model.

Corollary 1. *The disease-free equilibrium is locally asymptotically stable if* $\mathcal{R}_0 < 1$.

Corollary 2. *The endemic equilibrium is locally asymptotically stable if* $\mathcal{R}_0 > 1$.

Computing the Jacobian matrix of system (2.2) at the DFE yields the matrix in equation (3.12):

$$\mathcal{J}_f = \begin{pmatrix} k_1 & 0 & 0 & (1-d)z & -x & -y & -z & \delta \\ \alpha & -\mu & 0 & 0 & -a & -b & -c & 0 \\ 0 & 0 & k_3 & 0 & A & B & C & 0 \\ 0 & 0 & c & k_4 & 0 & 0 & 0 & 0 \\ 0 & 0 & fg & 0 & k_5 & 0 & 0 & 0 \\ 0 & 0 & (1-f)g & 0 & 0 & k_6 & 0 & 0 \\ 0 & 0 & 0 & dz & 0 & \eta & k_7 & 0 \\ 0 & 0 & 0 & 0 & r_1 & r_2 & r_3 & k_8 \end{pmatrix} \tag{3.12}$$

where:

$$\begin{aligned} &\beta_0 = \beta(1-\epsilon_m c_m)(1-s), \quad m = \frac{\Lambda}{\mu}, \\ &k_1 = -(\mu+\alpha), \quad k_3 = -(\mu+g+c), \quad k_4 = -(\mu+(1-d)z), \\ &k_5 = -(\mu+r_1), \quad k_6 = -(\mu+r_2+\eta), \quad k_7 = -(\mu+r_3), \quad k_8 = -(\mu+\delta), \\ &A = m\beta_0 + (1-\theta)m\beta_0, \quad a = (1-\theta)m\beta_0, \\ &b = (1-\theta)m\beta_0\epsilon_1, \quad c = (1-\theta)m\beta_0\epsilon_2, \\ &B = m\beta_0\epsilon_1 + (1-\theta)m\beta_0\epsilon_1, \\ &C = m\beta_0\epsilon_2 + (1-\theta)m\beta_0\epsilon_2, \\ &x = m\beta_0, \quad y = m\beta_0\epsilon_1, \quad z = m\beta_0\epsilon_2. \end{aligned}$$

The Gershgorin Circle Theorem (GCT) states that all eigenvalues of a matrix lie within at least one Gershgorin disc. Each disc D_i is centered at the diagonal entry a_{ii} of row i and has radius R_i, defined as the sum of the absolute values of the off-diagonal elements in that row:

$$D_i = \{z \in \mathbb{C} : |z - a_{ii}| \leq R_i\}, \quad \text{where} \quad R_i = \sum_{j \neq i} |a_{ij}|.$$

Computing the Gershgorin discs for the matrix $\mathcal{J}_f$:

- **First row:**
$$a_{11} = k_1 = -\mu, \quad R_1 = |(1-d)z| + |x| + |y| + |z| + |\delta|.$$
- **Second row:**
$$a_{22} = -\mu, \quad R_2 = |a| + |b| + |c|.$$
- **Third row:**
$$a_{33} = k_3, \quad R_3 = |A| + |B| + |C|.$$

- **Fourth row:**
$$a_{44} = k_4, \quad R_4 = |c|.$$

- **Fifth row:**
$$a_{55} = k_5, \quad R_5 = |fg|.$$

- **Sixth row:**
$$a_{66} = k_6, \quad R_6 = |(1-f)g|.$$

- **Seventh row:**
$$a_{77} = k_7, \quad R_7 = |dz| + |\eta|.$$

- **Eighth row:**
$$a_{88} = k_8, \quad R_8 = |r_1| + |r_2| + |r_3|.$$

Since all the Gershgorin discs lie entirely within the left half of the complex plane, it follows that all eigenvalues of $\mathcal{J}_f$ have negative real parts. Therefore, the disease-free equilibrium is locally asymptotically stable.

3.4.3 Global stability analysis of the DFE

We employ the quadratic Lyapunov function method to analyze the global asymptotic stability.

Theorem 3.5. ***(Global Stability via Quadratic Lyapunov Function)***
Consider the autonomous dynamical system given by:

$$\dot{x} = f(x),$$

where $x \in \mathbb{R}^n$ is the state vector, and $f : \mathbb{R}^n \to \mathbb{R}^n$ is a continuously differentiable function. Let x^* be an equilibrium point of the system, i.e., $f(x^*) = 0$.

Suppose there exists a quadratic Lyapunov function $V(x) : \mathbb{R}^n \to \mathbb{R}$ of the form

$$V(x) = (x - x^*)^\top P(x - x^*),$$

where P is a symmetric positive definite matrix, i.e., $P = P^\top > 0$, such that:

- ***Positive Definiteness:*** *$V(x) > 0$ for all $x \neq x^*$, and $V(x^*) = 0$.*

- ***Negative Definiteness of the Derivative:*** *The time derivative of $V(x)$ along the trajectories of the system, given by*
$$\dot{V}(x) = \frac{dV(x)}{dt} = \nabla V(x) \cdot f(x),$$
is negative definite, i.e., $\dot{V}(x) < 0$ for all $x \neq x^*$.

Conclusion: *If the above conditions are satisfied, then the equilibrium point x^* is globally asymptotically stable. That is, for any initial condition $x(0) \in \mathbb{R}^n$, the solution $x(t)$ converges to x^* as $t \to \infty$.*

The global stability analysis is carried out by constructing the Jacobian matrix of system (2.2) and evaluating it at the DFE, as shown in equation (3.13):

$$\mathcal{J}_f = \begin{pmatrix} k_1 & 0 & 0 & (1-d)z & -x & -y & -z & \delta \\ \alpha & -\mu & 0 & 0 & -a & -b & -c & 0 \\ 0 & 0 & k_3 & 0 & A & B & C & 0 \\ 0 & 0 & c & k_4 & 0 & 0 & 0 & 0 \\ 0 & 0 & fg & 0 & k_5 & 0 & 0 & 0 \\ 0 & 0 & (1-f)g & 0 & 0 & k_6 & 0 & 0 \\ 0 & 0 & 0 & dz & 0 & \eta & k_7 & 0 \\ 0 & 0 & 0 & 0 & r_1 & r_2 & r_3 & k_8 \end{pmatrix} \tag{3.13}$$

where:

$$\begin{aligned} &\beta_0 = \beta(1-\epsilon_m c_m)(1-s), \quad m = \frac{\Lambda}{\mu}, \\ &k_1 = -(\mu+\alpha), \quad k_3 = -(\mu+g+c), \quad k_4 = -(\mu+(1-d)z), \\ &k_5 = -(\mu+r_1), \quad k_6 = -(\mu+r_2+\eta), \quad k_7 = -(\mu+r_3), \quad k_8 = -(\mu+\delta), \\ &A = m\beta_0 + (1-\theta)m\beta_0, \quad a = (1-\theta)m\beta_0, \\ &b = (1-\theta)m\beta_0\epsilon_1, \quad c = (1-\theta)m\beta_0\epsilon_2, \\ &B = m\beta_0\epsilon_1 + (1-\theta)m\beta_0\epsilon_1, \\ &C = m\beta_0\epsilon_2 + (1-\theta)m\beta_0\epsilon_2, \\ &x = m\beta_0, \quad y = m\beta_0\epsilon_1, \quad z = m\beta_0\epsilon_2. \end{aligned}$$

A quadratic Lyapunov function of the form:

$$V(x) = x^\top P x$$

is considered, where $x = (x_1, x_2, x_3, x_4, x_5, x_6, x_7, x_8)^\top$, and P is a symmetric positive definite matrix. Let $P = I$, the identity matrix. Then, the Lyapunov function simplifies to:

$$V(x) = x_1^2 + x_2^2 + x_3^2 + x_4^2 + x_5^2 + x_6^2 + x_7^2 + x_8^2.$$

The time derivative of $V(x)$ along the system trajectories is:

$$\dot{V}(x) = \frac{d}{dt}(x^\top P x) = \dot{x}^\top P x + x^\top P \dot{x}.$$

Since $P = I$, we have:

$$\dot{V}(x) = \dot{x}^\top x + x^\top \dot{x} = 2x^\top \dot{x}.$$

Substituting $\dot{x} = Ax$, yields:

$$\dot{V}(x) = 2x^\top A x.$$

Thus,

$$\dot{V}(x) = 2\Big(k_1 x_1^2 + (1-d)z x_1 x_4 - m\beta_0 x_1 x_3 - \epsilon_1 m\beta_0 x_1 x_6 - \epsilon_2 m\beta_0 x_1 x_7 + \delta x_1 x_8 + \alpha x_1 x_2 - \mu x_2^2$$

$$+k_3x_3^2 + cx_3x_4 + k_4x_4^2 + fgx_3x_5 + k_5x_5^2 + (1-f)gx_3x_6 + k_6x_6^2 + dzx_4x_7 + \eta x_6x_7 + k_7x_7^2$$
$$+r_1x_5x_8 + r_2x_6x_8 + r_3x_7x_8 + k_8x_8^2\Big).$$

For global stability, $\dot{V}(x)$ must be negative definite, i.e., $\dot{V}(x) < 0$ for all $x \neq 0$. This condition is satisfied if all diagonal elements of the Jacobian are negative and the cross terms do not dominate.

To assess local stability of the disease-free equilibrium (DFE), the Gershgorin Circle Theorem was employed. This method provides a simple yet effective criterion for determining whether all eigenvalues of the Jacobian matrix have negative real parts. Biologically, this implies that if a small number of infections are introduced into the population, they will eventually die out, and the disease will not spread. Since none of the Gershgorin discs intersect the right half of the complex plane, all eigenvalues lie in the left half, confirming that the DFE is locally asymptotically stable.

In addition, a quadratic Lyapunov function was constructed to establish global stability under certain parameter conditions. The use of Lyapunov functions in epidemiological modeling is particularly valuable, as it enables verification of whether the system returns to a disease-free state, regardless of the initial infection size. This suggests that the combined interventions e.g., vaccination, quarantine, and face mask usage are not only effective in preventing outbreaks from small perturbations but also support long-term disease elimination when the reproduction number is kept below one.

Together, these mathematical tools offer a solid theoretical foundation for understanding how public health interventions can stabilize disease dynamics and facilitate sustained control or eradication efforts in real-world settings.

4 Bifurcation analysis

Bifurcation analysis plays a key role in determining parameter values or thresholds where the system undergoes qualitative changes in behavior. These changes can indicate shifts between disease-free states, endemic states, or even periodic outbreaks. Identifying such thresholds is essential for understanding, predicting, and managing disease dynamics.

Theorem 4.1. *(Theorem 4.1 of [7]). Consider the following general system of ordinary differential equations with a parameter ϕ:*

$$\frac{dx}{dt} = f(x,\phi), \quad f : \mathbb{R}^n \times \mathbb{R} \to \mathbb{R}, \quad f \in \mathrm{C}^2(\mathbb{R}^n \times \mathbb{R}). \tag{4.1}$$

Where 0 is an equilibrium point of the system (i.e., $f(0,\phi) = 0, \forall\phi$), and assume:

- *$A = D_x f(0,0) = \left[\frac{\partial f_i}{\partial x_j}(0,0)\right]$ is the linearization matrix of (4.1) around the equilibrium point 0, with ϕ evaluated at 0. Zero is a simple eigenvalue of A, and all other eigenvalues of A have negative real parts.*
- *Matrix A has a right eigenvector w and a left eigenvector v, each corresponding to the zero eigenvalue.*

Let f_k denote the k-th component of f, and define:

$$a = \sum_{k,i,j=1}^{n} v_k w_i w_j \frac{\partial^2 f_k}{\partial x_i \partial x_j}(0,0),$$

$$b = \sum_{k,i=1}^{n} v_k w_i \frac{\partial^2 f_k}{\partial x_i \partial \phi}(0,0).$$

The local dynamics of system (4.1) near the origin is fully determined by the signs of a and b:

(i) If $a > 0$, $b > 0$: when $\phi < 0$, with $|\phi| \ll 1$, the origin is locally asymptotically stable and a positive unstable equilibrium exists; when $0 < \phi \ll 1$, the origin is unstable and a locally asymptotically stable equilibrium emerges.

(ii) If $a < 0$, $b < 0$: when $\phi < 0$, the origin is locally asymptotically stable with a positive unstable equilibrium; when $\phi > 0$, the origin becomes unstable and a positive unstable equilibrium arises.

(iii) If $a > 0$, $b < 0$: when $\phi < 0$, the origin is unstable and a locally asymptotically stable negative equilibrium exists; when $\phi > 0$, the origin is stable and a positive unstable equilibrium appears.

(iv) If $a < 0$, $b > 0$: as ϕ changes from negative to positive, the origin changes its stability from stable to unstable. Correspondingly, a negative unstable equilibrium becomes positive and locally asymptotically stable.

Let the model system be written in the vector form:

$$\frac{dX}{dt} = G(X), \tag{4.2}$$

where

$$X = (x_1, x_2, x_3, x_4, x_5, x_6, x_7, x_8)^T, \quad G = (g_1, g_2, g_3, g_4, g_5, g_6, g_7, g_8).$$

So that $S = x_1, V = x_2, E = x_3, Q = x_4, A = x_5, I = x_6, J = x_7, R = x_8$. The model equations are represented in equations (4.3):

$$\begin{aligned}
\frac{dx_1}{dt} &= \Lambda + (1-d)zx_4 + \delta x_8 - (\alpha + \lambda + \mu)x_1,\\
\frac{dx_2}{dt} &= \alpha x_1 - (\mu + (1-\theta)\lambda)x_2,\\
\frac{dx_3}{dt} &= \lambda x_1 + (1-\theta)\lambda x_2 - (\mu + g + c)x_3,\\
\frac{dx_4}{dt} &= cx_3 - (\mu + z)x_4,\\
\frac{dx_5}{dt} &= fgx_3 - (\mu + r_1)x_5,\\
\frac{dx_6}{dt} &= (1-f)gx_3 - (\mu + r_2 + \eta)x_6,\\
\frac{dx_7}{dt} &= \eta x_6 + dzx_4 - (\mu + r_3)x_7,\\
\frac{dx_8}{dt} &= r_1x_5 + r_2x_6 + r_3x_7 - (\mu + \delta)x_8.
\end{aligned} \tag{4.3}$$

Let β be the bifurcation parameter. Setting $\mathcal{R}_0 = 1$ in equation (3.6) and solving for β yields:

$$\beta = \hat{\beta} = \frac{k_1k_2k_3k_4k_5}{m\left(cdz\epsilon_2k_3k_4 - k_2(fgk_4k_5 - (1-f)gk_3(k_5\epsilon_1 - \eta\epsilon_2))\right)}. \tag{4.4}$$

The disease-free equilibrium E_0 is locally stable when $\beta < \hat{\beta}$, and becomes unstable when $\beta > \hat{\beta}$. Consequently, $\hat{\beta}$ represents the bifurcation value.

The linearized matrix of system (2.2) at the disease-free equilibrium E_0, evaluated at $\beta = \hat{\beta}$, is:

$$\mathcal{J}(E_0|\hat{\beta}) = \begin{pmatrix} k_1 & 0 & 0 & (1-d)z & -x & -y & -z & \delta \\ \alpha & -\mu & 0 & 0 & -a & -b & -c & 0 \\ 0 & 0 & k_3 & 0 & A & B & C & 0 \\ 0 & 0 & c & k_4 & 0 & 0 & 0 & 0 \\ 0 & 0 & fg & 0 & k_5 & 0 & 0 & 0 \\ 0 & 0 & (1-f)g & 0 & 0 & k_6 & 0 & 0 \\ 0 & 0 & 0 & dz & 0 & \eta & k_7 & 0 \\ 0 & 0 & 0 & 0 & r_1 & r_2 & r_3 & k_8 \end{pmatrix} \tag{4.5}$$

where:

- $\beta_0 = \beta(1-\epsilon_m c_m)(1-s)$,
- $k_1 = -(\mu+\alpha)$, $k_2 = -\mu$, $k_3 = -(\mu+g+c)$, $k_4 = -(\mu+(1-d)z)$,
- $k_5 = -(\mu+r_1)$, $k_6 = -(\mu+r_2+\eta)$, $k_7 = -(\mu+r_3)$, $k_8 = -(\mu+\delta)$,
- $A = m\beta_0 + (1-\theta)m\beta_0$, $a = (1-\theta)m\beta_0$,
- $b = (1-\theta)m\beta_0\epsilon_1$, $c = (1-\theta)m\beta_0\epsilon_2$,
- $B = m\beta_0\epsilon_1 + (1-\theta)m\beta_0\epsilon_1$, $C = m\beta_0\epsilon_2 + (1-\theta)m\beta_0\epsilon_2$,
- $x = m\beta_0$, $y = m\beta_0\epsilon_1$, $z = m\beta_0\epsilon_2$,
- $m = \frac{\Lambda}{\mu}$.

The eigenvalues consist of seven real and negative values, along with a single zero eigenvalue, which can be determined using Wolfram Mathematica software as $k_1, k_2, k_3, k_4, k_5, k_6, k_6, k_7, k_8$. The zero eigenvalue is simple for the Jacobian matrix $\mathcal{J}(E_0|\hat{\beta})$, while the remaining eigenvalues are distinct and negative. Hence, the disease-free equilibrium (DFE), E_0, is a non-hyperbolic equilibrium, consistent with the assumption in Theorem 4.1 of [7].

Consequently, the center manifold theory can be utilized to analyze the local stability of the DFE, E_0. The right eigenvector, $m = (m_1, m_2, m_3, m_4, m_5, m_6, m_7, m_8)^T$, and the left eigenvector, $v = (v_1, v_2, v_3, v_4, v_5, v_6, v_7, v_8)$, corresponding to the simple zero eigenvalue of $\mathcal{J}(E_0|\hat{\beta})$, satisfy the condition $v \cdot m = 1$. These eigenvectors can be obtained by multiplying $v\mathcal{J}$ and $m\mathcal{J}$ and setting the resulting expressions equal to zero. The resulting system of the right eigenvalues

become;

$$\begin{aligned} m_1k_1 + m_4(1-d)z + m_5a_1 + m_6a_2 + m_7a_3 + m_8\delta = 0,\\ m_1\alpha + m_2k_2 + m_5a_4 + m_6a_5 + m_7a_6 = 0,\\ m_3k_3 + m_5b_1 + m_6b_2 + m_7b_3 = 0,\\ m_3c + m_4k_4 = 0,\\ m_3fg + m_5k_5 = 0,\\ m_3(1-f)g + m_6k_6 = 0,\\ m_4dz + m_6\eta + m_7k_7 = 0,\\ m_5r_1 + m_6r_2 + m_7r_3 + m_8k_8 = 0. \end{aligned} \tag{4.6}$$

From the equation 4.6 above:

Let $m_3 > 0$, then:

$$\begin{aligned} &m_4 = \frac{cm_3}{k_4}, \quad m_5 = \frac{fgm_3}{k_5},\\ &m_6 = \frac{(1-f)gm_3}{k_6}, \quad m_7 = -\left(\frac{(1-f)gm_3}{k_6} + \frac{c}{k_4}\right)\frac{m_3}{k_7},\\ &m_8 = -\frac{1}{k_8}(m_5r_1 + m_6r_2 + m_7r_3), \quad m_1 = -\frac{1}{k_1}(m_4(1-d)z + m_5a_1 + m_6a_2 + m_7a_3 + m_8\delta),\\ &m_2 = -\frac{1}{k_2}(m_1\alpha + m_5a_4 + m_6a_5 + m_7a_6). \end{aligned} \tag{4.7}$$

Also, the left eigenvector $v = (v_1, v_2, v_3, v_4, v_5, v_6, v_7, v_8)$, corresponding to the zero eigenvalue is obtained from $\mathcal{J}(E_0|\hat{\beta}) = 0$, which yields;

$$\begin{aligned} v_1k_1 + v_2\alpha = 0,\\ v_2k_2 = 0,\\ v_3k_3 + v_4c + v_5fg + v_6(1_f)g = 0,\\ v_1(1_d)z + v_4k_4 + v_7dz = 0,\\ -v_1x - v_2a - v_3A + v_5k_5 + v_8r_1 = 0,\\ -v_1y - v_2b - v_3B + v_6k_+v_7\eta + v_8r_2 = 0,\\ -v_1x - v_2c - v_3C + v_7k_7 = 0,\\ v_1\delta + v_8k_8 = 0. \end{aligned} \tag{4.8}$$

From equation 4.8 above, $v_1 = v_2 = v_8 = 0$. Then,

$$\begin{aligned} let, v_4 = v_4 > 0, then; v_7 = \frac{-k_4v_4}{dz},\\ v_3 = \frac{k_7k_4v_4}{b_3dz},\\ v_5 = \frac{-(b_1k_7k_4v_4)}{dzb_3k_5},\\ v_6 = -\frac{v_3b_2 + v_7\eta}{k_6}. \end{aligned} \tag{4.9}$$

To satisfy the condition $v.m = 1$, we determine the value of v_2. To compute the bifurcation

coefficients a and b as defined in Theorem 4.1, we consider system model 2.1 in the following form:

$$\frac{dX}{dt} = f = (f_1, f_2, f_3, f_4, f_5, f_6, f_7, f_8)^T \tag{4.10}$$

where $X = (x_1, x_2, x_3, x_4, x_5, x_6, x_7, x_8)^T$.
The coefficients a and b are derived from the partial derivatives in equations 33 and 35, respectively.

$$a = \sum_{k,i,j=1}^{8} v_k m_i m_j \frac{\partial^2 f_k}{\partial x_i \partial x_j}(0,0), \tag{4.11}$$

and

$$b = \sum_{k,i=1}^{8} v_k m_i \frac{\partial^2 f_k}{\partial x_i \partial \hat{\xi}}(0,0). \tag{4.12}$$

Since the components v_1, v_2, and v_8 are zero, it is unnecessary to compute the derivatives of f_1, f_7, and f_8. Among the derivatives of the remaining functions f_3, f_4, f_5, f_6, and f_7, only those with non-zero partial derivatives are taken into account, such that:

$$\begin{aligned}
&\frac{\partial^2 f_3}{\partial x_1 \partial x_5} = \frac{\partial^2 f_3}{\partial x_5 \partial x_1} = 1, && \frac{\partial^2 f_3}{\partial x_1 \partial x_7} = \frac{\partial^2 f_3}{\partial x_7 \partial x_1} = \epsilon_2,\\
&\frac{\partial^2 f_3}{\partial x_1 \partial x_6} = \frac{\partial^2 f_3}{\partial x_6 \partial x_1} = \epsilon_1, && \frac{\partial^2 f_3}{\partial x_2 \partial x_5} = \frac{\partial^2 f_3}{\partial x_5 \partial x_2} = (1-\theta),\\
&\frac{\partial^2 f_3}{\partial x_2 \partial x_6} = \frac{\partial^2 f_3}{\partial x_6 \partial x_2} = (1-\theta)\epsilon_1, && \frac{\partial^2 f_3}{\partial x_2 \partial x_7} = \frac{\partial^2 f_3}{\partial x_7 \partial x_2} = (1-\theta)\epsilon_2.
\end{aligned} \tag{4.13}$$

Considering the study of [6], the indication of whether a forward or backward bifurcation occurs is determined by the parameter a. Consequently, this yields Equation (32):

$$\begin{aligned}
a = {} & 2v_5 m_1 m_5 + 2v_3 m_1 m_7 \epsilon_2 + 2v_3 m_1 m_6 \epsilon_1 + 2v_3 m_1 m_5 (1-\theta)\\
& + 2v_3 m_1 m_7 (1-\theta)\epsilon_2 + 2v_3 m_1 m_6 (1-\theta)\epsilon_1 > 0.
\end{aligned} \tag{4.14}$$

Therefore, a mathematical system consisting of equations, as presented in Equation (2.2), exhibits a **forward bifurcation** at $\mathcal{R}_0 = 1$, given that $\beta > \hat{\beta}$ (representing the effective contact rate). The bifurcation analysis of the model reveals the occurrence of a forward bifurcation at the critical threshold where the basic reproduction number $\mathcal{R}_0 = 1$.

In epidemiological terms, a forward bifurcation implies that the disease-free equilibrium is stable when $\mathcal{R}_0 < 1$, and an endemic equilibrium emerges and becomes stable only when $\mathcal{R}_0 > 1$. This behavior suggests that bringing $\mathcal{R}_0$ below unity is both necessary and sufficient for disease elimination.

From a public health perspective, this means that intervention strategies—such as mass vaccination, early detection and isolation of cases, and widespread use of face masks—can effectively reduce the reproduction number below the critical threshold and lead to disease eradication. Moreover, the absence of a backward bifurcation indicates that there is no risk of disease persistence when $\mathcal{R}_0 < 1$, which simplifies control efforts and emphasizes the importance of early and sustained interventions to maintain this condition.

5 Sensitivity analysis

To determine the most efficient intervention program, sensitivity analysis plays a key role in decision-making. While disease transmission is related to R_0, the prevalence of the disease is

related to the endemic equilibrium. Sensitivity indices provide insights into the significance of each parameter in influencing disease transmission and prevalence.

A parameter with a higher index indicates a greater influence and should thus be prioritized for regulation. A negative sensitivity index implies that increasing the parameter value leads to a reduction in disease prevalence and transmission, whereas a positive index suggests that an increase in the parameter will result in increased transmission and prevalence.

We conducted a sensitivity analysis following the method proposed by [9] and further elaborated by [23]. The analysis used the *normalized forward sensitivity index*, defined as follows:

$$S_n = \frac{\partial R_0}{\partial \nu} \cdot \frac{\nu}{R_0}, \tag{5.1}$$

where ν represents a model parameter.

The table below shows the sensitivity indices of the parameters used:

Table 5.1: Sensitivity indices of model parameters

Symbol	**Sensitivity Index**
d	0.001
z	0.001
c	-0.0744
f	0.4125
g	0.7325
η	0.0004
ϵ_m	-0.3158
c_m	-0.32
s	-0.4286
μ	-2.5607
Λ	1
β	1

6 Numerical simulations

To analyze the impact of various interventions on the prevention and management of respiratory infections, numerical simulations were performed using System Model 1. The model utilized parameter values derived from existing studies, with certain estimates made to ensure meaningful analysis in this context.

For this study, the parameter values listed in Table 1 were used for the simulations, which spanned a time period of $0 \leq t \leq 100$ days, representing the expected timeframe for the disease to complete its course. The simulations were carried out using Python, with Jupyter Notebook serving as the integrated development environment (IDE). The results are presented graphically.

6.1 Numerical simulation on the impact of vaccination rate and efficacy

Increasing the vaccination rate, as illustrated in Figure 6.1, significantly reduces the number of symptomatic infections, as more individuals are immunized before being exposed to the disease. Higher vaccination rates also shift the timing of peak infections earlier, indicating quicker control of the outbreak. Furthermore, the magnitude of peak infections decreases with faster vaccination, demonstrating the effectiveness of immunization in curbing disease transmission. Ultimately, higher vaccination rates accelerate the decline in infections, leading to a shorter epidemic duration and improved overall containment.

The simulation in Figure 6.2 demonstrates that higher vaccine efficacy leads to a substantial reduction in the number of symptomatic infections (I), emphasizing the importance of developing and administering highly effective vaccines. As vaccine efficacy increases, the peak of symptomatic infections becomes smaller and occurs earlier, indicating faster and more effective disease control. Lower efficacy results in higher infection peaks and prolonged disease spread, highlighting the vulnerability of the population when vaccine performance is suboptimal. Overall, improving vaccine efficacy significantly mitigates the severity and duration of the outbreak, underlining its critical role in managing infectious diseases, as illustrated in Figure 6.2.

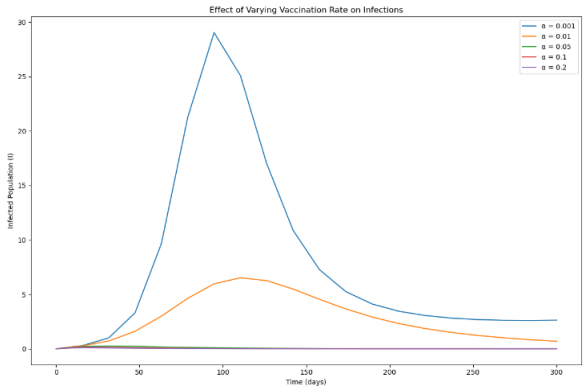

Figure 6.1: Effect of varying vaccination rate

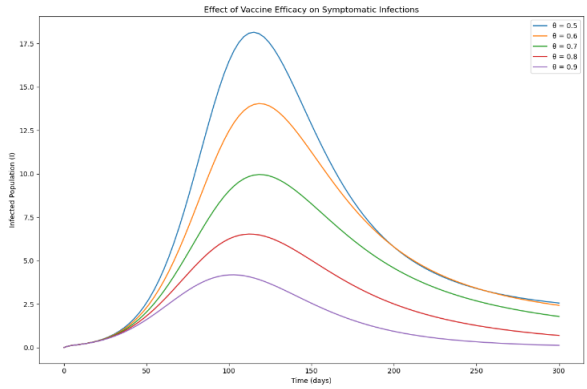

Figure 6.2: Effect of varying vaccination efficacy

6.2 Numerical simulation on the impact of face mask compliance

The simulation in Figure 6.3 reveals that increasing face mask compliance (ϵ_m) significantly reduces the peak and overall size of the symptomatic infected population (I), demonstrating the effectiveness of masks in controlling disease spread. With higher compliance, the infection curve flattens and peaks later, highlighting the role of masks in delaying and mitigating outbreaks. Low or no compliance leads to a sharp and higher infection peak, overwhelming public health systems, while full compliance achieves maximum reduction in infections. These results underscore the critical importance of widespread mask usage as a simple yet powerful intervention in infectious disease management.

6.3 Numerical simulation on the impact of consistent face mask use

The simulation in Figure 6.4 demonstrates that consistent mask-wearing, with an 80% reduction in effective transmission, substantially lowers both symptomatic (I) and asymptomatic (A) infections over time. Symptomatic infections show a notable peak followed by a steady decline, while asymptomatic infections maintain a lower profile throughout the simulation, indicating masks' significant impact on reducing disease spread. The reduced transmission also delays the infection peaks, offering additional time for healthcare systems to manage cases and implement further interventions. Overall, consistent mask-wearing proves to be an effective strategy in controlling the outbreak and minimizing the burden of symptomatic cases.

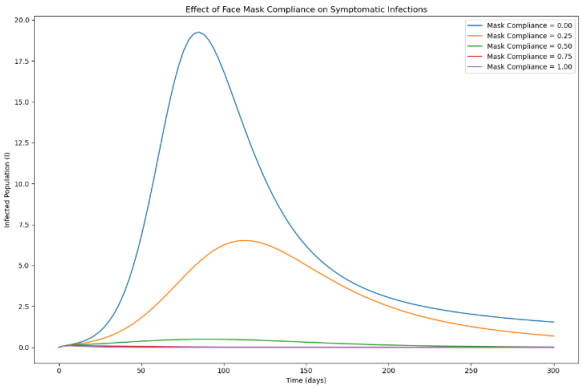

Figure 6.3: Effect of varying mask compliance

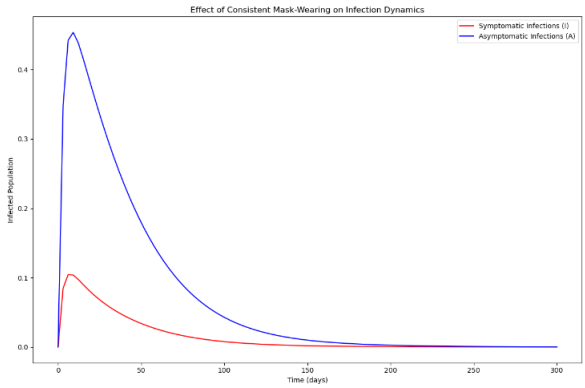

Figure 6.4: Effect of varying consistent mask use

6.4 Numerical simulation on the impact of quarantine

The simulation in Figure 6.5 highlights the critical role of quarantine in mitigating infection dynamics, with quarantined individuals (Q) peaking shortly after the rise in exposed (E) and asymptomatic (A) infections. Symptomatic infections (I) experience a delayed and lower peak compared to models without quarantine, demonstrating its effectiveness in reducing transmission. The exposed compartment steadily decreases as individuals are quarantined, while asymptomatic and symptomatic cases remain controlled due to timely isolation measures. Overall, the implementation of quarantine effectively suppresses the outbreak by breaking chains of transmission and reducing the burden on the susceptible population.

7 Conclusion

This study developed and analyzed a novel mathematical model that integrates vaccination, quarantine, and face mask usage to assess their collective impact on the transmission dynamics of infectious respiratory diseases. The model provides a unified framework to evaluate the effectiveness of these public health interventions both analytically and numerically.

Through rigorous stability analysis using the Gershgorin Circle Theorem and global stability techniques, the disease-free equilibrium (DFE) was shown to be locally asymptotically stable under appropriate conditions. Bifurcation analysis further confirmed the presence of a

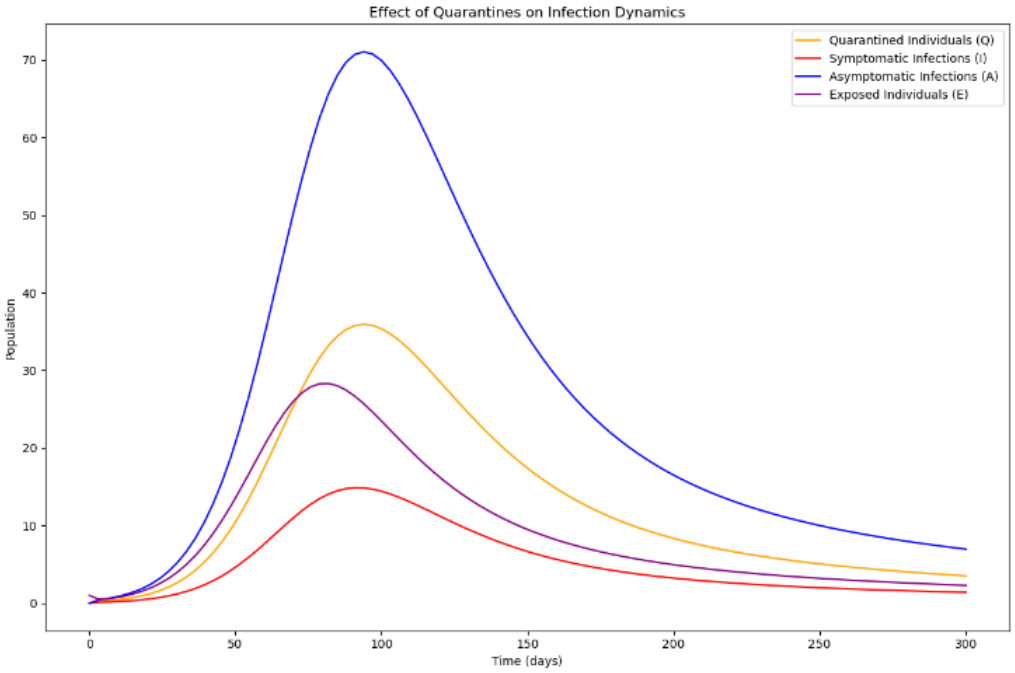

Figure 6.5: Effect of applying quarantine

forward bifurcation, indicating that the disease can be eradicated when the basic reproduction number is brought below one through targeted interventions.

Numerical simulations and sensitivity analysis revealed that certain parameters particularly the contact rate, vaccination rate, and mask compliance play a critical role in determining the progression and control of the disease. These findings underscore the importance of strengthening and maintaining a combination of public health measures rather than relying on a single intervention strategy. Specifically, the results suggest that high compliance with mask usage, increased vaccine coverage, and effective quarantine procedures work synergistically to reduce the basic reproduction number and suppress disease outbreaks.

Compared to existing models, which often analyze these interventions in isolation, this study contributes a more holistic perspective by simultaneously incorporating multiple layers of disease control. The sensitivity analysis offers practical insights for policymakers by identifying the most influential parameters to target when designing intervention strategies. Furthermore, the deterministic framework employed ensures computational efficiency and interpretability, making the model suitable for use in informing real-time decision-making.

Declarations

Availability of data and materials

Not applicable

Funding

Not applicable

Authors' contributions

All the authors have contributed equally to this paper

Conflict of interest

The authors have no conflicts of interest to declare.

References

[1] M. O. Adeniyi, M. I. Ekum, C. Iluno, and S. I. Oke, *Dynamic model of COVID-19 disease with exploratory data analysis*, Scientific African, **9** (2020), e00477.

[2] A. A. Alimi and A. A. Ayoade, *Mathematical modeling of the effect of vaccination on the dynamics of infectious diseases*, Nepal Journal of Mathematical Sciences, **4**(1) (2023), 110.

[3] A. S. Alsheri, A. A. Alraeza, and M. R. Afia, *Mathematical modeling of the effect of quarantine rate on controlling the infection of COVID-19 in the population of Saudi Arabia*, Alexandria Engineering Journal, **61**(9) (2022), 68436850.

[4] G. Birkhoff and G. C. Rota, *Ordinary Differential Equations*, Blaisdell Pub. Co., Waltham, Mass, 1969.

[5] V. Bitsouni, N. Gialelis, and I. G. Stratis, *A model for the outbreak of COVID-19: Vaccine effectiveness in a case study of Italy*, arXiv preprint arXiv:2008.00828, 2020.

[6] B. Buonomo and C. Vargas-De-León, *Stability and bifurcation analysis of a vector-bias model of malaria transmission*, Mathematical Biosciences and Engineering, **242**(1) (2013), 5967. https://doi.org/10.1016/j.mbs.2012.12.001

[7] C. Castillo-Chavez and B. Song, *Dynamical models of tuberculosis and their applications*, Mathematical Biosciences and Engineering, **1**(2) (2004), 361404. https://doi.org/10.3934/mbe.2004.1.361

[8] K. H. Chan and K.-Y. Yuen, *COVID-19 epidemic: disentangling the re-emerging controversy about medical facemasks from an epidemiological perspective*, International Journal of Epidemiology, **49**(4) (2020), 10631066.

[9] N. Chitnis, J. M. Hyman, and J. M. Cushing, *Determining important parameters in the spread of malaria through the sensitivity analysis of a mathematical model*, Bulletin of Mathematical Biology, **70**(5) (2008), 12721296.

[10] C. Connelly, *Epidemiology Through the Lens of Differential Equations*, 2023.

[11] S. E. Eikenberry, M. Mancuso, E. Iboi, T. Phan, K. Eikenberry, Y. Kuang, E. Kostelich, and A. B. Gumel, *To mask or not to mask: Modeling the potential for face mask use by the general public to curtail the COVID-19 pandemic*, Infectious Disease Modelling, **6**(1) (2020), 293308.

[12] N. K. Geofrey, M. Harun, M. Samuel, and N. Edward, *A Mathematical Model to Investigate How Vaccination Affect the Reproduction Number for COVID-19*, International Journal of Systems Science and Applied Mathematics, **9**(2) (2024), 2029. https://doi.org/10.11648/j.ijssam.20240902.11

[13] Y. Gu, S. Ullah, M. A. Khan, M. Y. Alshahrani, M. Abohassan, and M. B. Riaz, *Mathematical modeling and stability analysis of the COVID-19 with quarantine and isolation*, Results in Physics, **34** (2022), 105284.

[14] I. U. Haq, N. Ullah, N. Ali, and K. S. Nisar, *A new mathematical model of COVID-19 with quarantine and vaccination*, Mathematics, **11**(1) (2022), 142.

[15] L. P. James, J. A. Salomon, C. O. Buckee, and N. A. Menzies, *The use and misuse of mathematical modeling for infectious disease policymaking: lessons for the COVID-19 pandemic*, Medical Decision Making, **41**(4) (2021), 379385. https://doi.org/10.1007/s11071-011-0263-4

[16] Q. Li, X. Guan, P. Wu, X. Wang, L. Zhou, Y. Tong, ... and Z. Feng, *Early transmission dynamics in Wuhan, China, of novel coronavirusinfected pneumonia*, New England Journal of Medicine, **382**(13) (2020), 11991207.

[17] C. R. MacIntyre and A. A. Chughtai, *Facemasks for the prevention of infection in healthcare and community settings*, BMJ, **350** (2015).

[18] S. Mandal, N. Arinaminpathy, B. Bhargava, and S. Panda, *Plausibility of a third wave of COVID-19 in India: a mathematical modelling based analysis*, The Indian Journal of Medical Research, **153**(5-6) (2021), 522.

[19] N. Nuraini, K. K. Sukandar, P. Hadisoemarto, H. Susanto, A. I. Hasan, and N. Sumarti, *Mathematical models for assessing vaccination scenarios in several provinces in Indonesia*, Infectious Disease Modelling, **6** (2021), 12361258. https://doi.org/10.1016/j.idm.2021.09.002

[20] J. N. Paul, I. S. Mbalawata, S. S. Mirau, and L. Masandawa, *Mathematical modeling of vaccination as a control measure of stress to fight COVID-19 infections*, Chaos, Solitons and Fractals, **166** (2023), 112920.

[21] C. Rattanakul and I. Chaiya, *A mathematical model for predicting and controlling COVID-19 transmission with impulsive vaccination*, AIMS Mathematics, **9**(4) (2024), 62816304.

[22] H. M. Wanjala, M. O. Okongo, and J. O. Ochwach, *Mathematical Model of the Impact of Home-Based Care on Contagious Respiratory Illness Under Optimal Conditions*, Jambura Journal of Biomath, **5**(2) (2024), 8394. https://doi.org/10.37905/jjbm.v5i2.27611

[23] H. M. Wanjala, *Mathematical Modelling of SARS-CoV-2 Incorporating Non-Pharmaceutical Interventions Coupled with Vaccination*, Masters thesis, Chuka University, 2023. https://doi.org/10.13140/RG.2.2.35446.78405

[24] H. M. Wanjala, M. O. Okongo, and J. O. Ochwach, *Impact of Media Awareness and Use of Face-Masks on Infectious Respiratory Disease*, Pan-American Journal of Mathematics, **2** (2023), 15.